Title

Inhibitory synaptic transmission differs in mouse type A and B medial vestibular nucleus neurons, *in vitro*

Authors

Aaron J. Camp, Robert J. Callister, Alan M. Brichta

Address

School of Biomedical Sciences & Hunter Medical Research Institute, Faculty of Health

The University of Newcastle,

Callaghan, NSW 2308,

Australia.

Corresponding author

Alan M. Brichta,

School of Biomedical Sciences, Faculty of Health,

The University of Newcastle, Callaghan, NSW 2308, Australia

+ 61 2 4921 7026 phone

+ 61 2 4921 8667 fax

Alan.Brichta@newcastle.edu.au

Running title

Inhibitory synaptic transmission in MVN neurons

ABSTRACT

Fast inhibitory synaptic transmission in the medial vestibular nucleus (MVN) is mediated by $GABA_A$ receptors ($GABA_ARs$) and glycine receptors (GlyRs). To assess their relative contribution to inhibition in the MVN, we recorded miniature inhibitory postsynaptic currents (mIPSCs) in physiologically characterized type A and type B MVN neurons. Transverse brainstem slices were prepared from mice (3-8 weeks old) and whole-cell patch-clamp recordings were obtained from visualized MVN neurons (CsCl internal; V_m = –70 mV; 23°C). In 81 MVN neurons, 69% received exclusively $GABA_A$ergic inputs, 6% exclusively glycinergic inputs, and 25% received both types of mIPSCs. The mean amplitude of $GABA_AR$-mediated mIPSCs was smaller than those mediated by GlyRs (22.6 ± 1.8 vs. 35.3 ± 5.3 pA). The rise time and decay time constants of $GABA_AR$- vs. GlyR-mediated mIPSCs were slower (1.3 ± 0.1 vs. 0.9 ± 0.1 ms and 10.5 ± 0.3 vs. 4.7 ± 0.3 ms respectively). Comparison of type A (n = 20) and type B (n = 32) neurons showed that type A neurons received almost exclusively $GABA_A$ergic inhibitory inputs, whereas type B neurons received $GABA_A$ergic inputs, glycinergic inputs or both. Intracellular labeling in a subset of MVN neurons showed that morphology was not related to a MVN neuron's inhibitory profile (n = 15), or whether it was classified as type A or B (n = 29). Together, these findings indicate that: 1) both GABA and glycine contribute to inhibitory synaptic processing in MVN neurons, although GABA dominates; and 2) there is a difference in the distribution of $GABA_A$ and Gly receptors between Type A and Type B MVN neurons.

INTRODUCTION

Medial vestibular nucleus (MVN) neurons are a major central target for afferents originating in the horizontal semicircular canal, and their projections play an important role in reflex control of eye and head movement (for review see Wilson and Melvill Jones 1979). MVN neurons are tonically active and their output is synaptically modulated by vestibular afferent input, reciprocal connections with contralateral vestibular nuclei, and inputs from cerebellar Purkinje cells (for review see Barmack 2003; Smith and Curthoys 1989). These synaptic inputs are crucial for motor learning within the vestibulo-ocular reflex, and the plasticity that occurs following peripheral vestibular lesions (Curthoys and Halmagyi 1995; Darlington and Smith 2000).

The contribution of fast inhibitory synaptic transmission in modulating MVN neuron output remains unclear, as few studies have directly examined the properties of inhibitory amino acid receptors in any vestibular nucleus neurons, mammalian (Chun et al. 2003), or non-mammalian (Straka and Dieringer 1996; Shao et al. 2004, 2003), for review see Straka et al. 2005. In mammals it is known that activation of γ-aminobutyric acid receptors ($GABA_A$ receptors) is important in the commissural pathway that connects medial vestibular nuclei on either side of the brainstem (Furuya et al. 1991; Shimazu and Precht 1966), and in cerebello-vestibular circuitry (Babalian and Vidal 2000; Cox and Peusner 1990; du Lac and Lisberger 1992). Also, application of the $GABA_A$ receptor agonist muscimol leads to a dose-dependent decrease in the resting discharge of MVN neurons (Johnston et al. 2001; Yamanaka et al. 2000). Furthermore, changes in $GABA_A$ receptor responsiveness have been

implicated in the recovery of resting activity in ipsilesional MVN neurons following unilateral labyrinthectomy (Cameron and Dutia 1997; Johnston et al. 2001; Yamanaka et al. 2000).

Both GABA and glycine immunoreactive neurons, and $GABA_A$ and glycine receptors, have been identified in the MVN (Eleore et al. 2005; Eleore et al. 2004; Horii et al. 2004; Spencer and Baker 1992; Takazawa et al. 2004; Vibert et al. 2000). Despite this, most electrophysiological data regarding inhibitory synaptic transmission in the MVN has focused on the effect of $GABA_A$ agonists on MVN neuron discharge (Johnston et al. 2001; Yamanaka et al. 2000). No studies have addressed the contribution of glycine acting at functional synaptic connections in modulating MVN output, although application of glycine has also been shown to decrease spontaneous discharge in MVN neurons (Lapeyre and De Waele 1995; Precht et al. 1973; Vibert et al. 2000).

Recordings in *in vitro* slice preparations have shown that MVN neurons remain tonically active and can be classified into two major types according to the properties of their action potential afterhyperpolarization (AHP) (Beraneck et al. 2003; Gallagher et al. 1985; Johnston et al. 1994; Serafin et al. 1991). Type A MVN neurons display a large-amplitude, monophasic AHP, whereas type B neurons show a smaller amplitude, biphasic AHP. The varied action potential properties of MVN neurons, including AHP shape, are thought to be due to differences in intrinsic membrane properties (for review Goldberg 2000). When combined with the effects of synaptic inputs, these intrinsic properties allow regulation of MVN discharge in response to a diverse range of head movements.

In the present study we used whole cell recording techniques to examine $GABA_A$ergic and glycinergic inhibitory synaptic transmission in mouse MVN neurons. Using a combination of voltage- and current-clamp techniques we tested whether $GABA_A$ergic and glycinergic transmission differed in the two major physiological classes of MVN neurons (types A and B). Eighty-one of ninety-six recorded neurons displayed resolvable mIPSCs, and of these neurons, most (69%) expressed exclusively $GABA_A$ receptors, 6% expressed exclusively glycine receptors, and 25% expressed both types of receptor.

MATERIALS AND METHODS

Tissue preparation

Mice (C57/Bl6 strain, both sexes) aged 3-8 wks were used in this study. These ages were chosen since by the beginning of postnatal week three (P15) MVN neurons display intrinsic electrophysiological properties that allow identification of type A and type B neurons (Dutia and Johnston 1998). All procedures were in accordance with The University of Newcastle's animal care and ethics committee guidelines. Mice were deeply anaesthetized with an intra-peritoneal injection of Ketamine (100 $mg \bullet kg^{-1}$) and decapitated. The parietal, and part of the occipital bone were removed together with the cerebellum to expose the brainstem. To maintain tissue viability throughout this procedure, the brain and brainstem were constantly bathed in ice-cold sucrose-modified artificial cerebrospinal fluid sACSF containing (in mM): 236 Sucrose, 25 $NaHCO_3$, 11 Glucose, 2.5 KCl, 1 NaH_2PO_4, 1 $MgCl_2$ and 2.5 $CaCl_2$ (Graham et al. 2003). This solution was continually gassed with Carbogen (95% O_2, 5% CO_2) to achieve a final pH of 7.2-7.3. The brainstem (inferior colliculi to obex) was then isolated and removed from the surrounding bone. The excised brainstem was mounted on a styrofoam block, rostral end down, secured to the stage of a vibrating microtome (VT1000s, Leica Microsystems, Nuslock, Germany) using cyanoacrylate glue (Loctite 454, Loctite, Caringbah, Australia), and transferred to a cutting chamber filled with ice-cold sACSF. Slices (300 µm thick) were cut, and those containing the MVN (5-6 slices extending from hypoglossal nuclei to facial nerve) were transferred to an incubation chamber and allowed to equilibrate for ~1hr before recording.

Electrophysiology

Following incubation, slices were transferred to a small glass-bottom recording chamber and held in place by nylon threads fixed to a U-shaped flattened platinum wire. The chamber was continually perfused with ACSF (118 mM NaCl substituted for sucrose in sACSF) at room temperature (21-23°C). This temperature was selected in order to compare receptor kinetics with the large $GABA_A$/glycine receptor literature. Furthermore a recent study by Takazawa et al. (2004) concluded that although spike parameters may be affected at room temperature, changes in the classification of MVN neurons is unlikely. Slices were viewed via a fixed-stage microscope (BX51WI, Olympus, Tokyo, Japan) at low power (4X) to identify the MVN. Near infra-red differential interference contrast (IR-DIC) optics and a 40X water-immersion lens were used for visualizing individual MVN neurons. Positioning of the recording electrode was controlled using a motorized manipulator (Model MS-314, Marzhauser Wetzlar, Wetzlar-Steindorf, Germany).

Recording electrodes (2-4 MΩ resistance) were pulled from borosilicate glass tubing (1.5 mm o.d., Harvard Apparatus, Kent, UK) on a Brown Flaming P-97 micropipette puller (Sutter Instruments, Novato, CA). For characterizing miniature inhibitory postsynaptic currents (mIPSCs), pipettes were filled with an internal electrode solution containing (in mM): 130 CsCl, 10 HEPES, 10 EGTA, 1 $MgCl_2$, 2 ATP, and 0.3 GTP (pH adjusted to 7.3 with 1M CsOH). To assess the effects of Cs-based internal solution on action potential (AP) properties, we compared APs with those recorded in a potassium-based internal solution containing (in mM): 135 $KMeSO_4$, 8 NaCl, 10 HEPES, 0.1 EGTA, 2 Mg_2ATP, 0.3 Na_3GTP (pH adjusted to 7.3 with 1 M KOH). For mIPSCs, whole cell recordings were amplified and filtered (2 KHz) using

an Axopatch 1D amplifier (Axon Instruments, Foster City, CA). Signals were captured (10 K samples/s) using an Apple Macintosh G4 computer, an ITC-16i Analogue/Digital converter (Instrutech, Long Island, NY) and Axograph v4.8 data acquisition software (Axon Instruments, Foster City, CA).

Experimental protocol

mIPSC Recordings Whole-cell voltage-clamp was used to record mIPSCs. After forming a high resistance seal (> 1 GΩ) on the soma of an IR-DIC visualized MVN neuron, the whole-cell recording configuration was established by applying brief suction to the pipette tip. Series and input resistance were calculated from the response to a 10 mV hyperpolarizing voltage step from a holding potential of –70 mV. Input resistance was monitored throughout each experiment by presenting this pulse every 10 seconds. Data were rejected if the series resistance changed by more than 20% during the course of an experiment. Changes in input resistance, on the other hand, were not used as a criterion for excluding neurons since this parameter could be affected by receptor blockade. Series resistance and membrane capacitance were uncompensated. In voltage-clamp, using CsCl internal, $GABA_A$- and glycine-mediated mIPSCs were pharmacologically isolated by adding 6-cyano-7-nitroquinoxaline-2-3-dione (CNQX, 10 μM) and tetrodotoxin (TTX; 1 μM) to block AMPA-kainate type glutamate receptors and voltage-activated sodium channels, respectively. These blockers were added after characterization of AP properties. mIPSCs recorded under these conditions represent combinations of $GABA_A$ receptor ($GABA_AR$)- and glycine receptor (GlyR)-mediated mIPSCs. The $GABA_AR$ antagonist bicuculline (10 μM) was then added to the bath. If all mIPSCs were abolished following the addition of bicuculline, the previously recorded mIPSCs were

classified as being exclusively $GABA_A$ergic. mIPSCs that remained following addition of bicuculline were classed as glycinergic and this was confirmed by the abolition of all activity using the GlyR antagonist, strychnine (1 μM). In a limited number of neurons the order of inhibitory antagonist application was reversed (strychnine prior to bicuculline). Altering the conditions in this way did not change $GABA_A$ or glycine receptor kinetics. All mIPSC experiments were carried out at a holding potential of –70 mV to block n-methy-d-aspartate (NMDA) glutamate receptors. At least three minutes of data were used for analysis of the various types of mIPSC. To pharmacologically isolate $GABA_A$ or glycine receptor mediated mIPSCs required between 11-16 minutes in total. In cases where more than one cell was recorded per slice, at least 30 minutes was allowed to ensure drug washout. TTX was obtained from Alomone Laboratories (Jerusalem, Israel). All other drugs were obtained from Sigma Chemicals (St Louis, MO).

mIPSCs recorded in type A and B MVN neurons

One of the major aims of this study was to examine the contribution of $GABA_A$ergic and glycinergic transmission in type A and B MVN neurons. The use of a CsCl internal solution in the recording pipette is a well-accepted method for recording mIPSCs (Graham et al. 2003; Lim et al. 2003; Singer et al. 1998), and allows direct comparison of kinetics with previous studies of $GABA_A$/glycine receptors. However, use of a CsCl internal solution presents difficulties when recording and analyzing action potential properties, as cesium ions block potassium channels, which are responsible for features of the AP including the AHP (see Hille 2001). In order to study mIPSC and action potential properties in the **same** neuron we adapted the recently described method of Hefti and Smith (2003) to analyze AP characteristics in

recordings obtained with a CsCl internal solution (Fig. 1). According to this technique, APs recorded **immediately** after switching from cell-attached to the whole-cell recording configuration (breakthrough; arrow in Fig. 1B) can be used for analysis of AP characteristics. During this period, the CsCl-based internal solution has not fully dialyzed the cell and therefore intrinsic membrane conductances have not been dramatically altered. In our hands it was possible to classify a majority of MVN neurons based on their AP shape (described below), one to five seconds after breakthrough. This allowed classification of **both** AP properties and mIPSC characteristics.

Recordings obtained in a typical experiment involved first establishing a gigaohm seal on a visualized MVN neuron in voltage clamp mode (see Fig. 1). The amplifier was then switched to current clamp mode. In some cases occasional extracellular APs were observed under these conditions (Fig. 1A1). In later experiments this activity was allowed time (2-5 min) to become more regular, and served as an indicator for achieving successful whole cell current clamp configuration. In current clamp the tonic AP discharge, a characteristic of MVN neurons, was now observed (Fig. 1A2). Typically, APs recorded immediately following breakthrough were characterized by a robust overshoot (more positive than +20mV), and a deep AHP (more negative than –60mV). As might be expected, cesium diffusing from the pipette into the neuron, gradually increased AP discharge rate and attenuated spike height (Fig. 1B). After ~ 6 - 30 s the amplifier was switched to voltage clamp and the holding potential set to –70 mV for subsequent characterization of mIPSCs (Fig. 1A3). These mIPSCs were then pharmacologically dissected into $GABA_A$ergic or glycinergic components for subsequent analysis.

Data analysis

mIPSC analysis Both classes of mIPSCs were analyzed offline using a semi-automated, sliding template protocol within the Axograph analysis package (Clements and Bekkers 1997). A detection criterion was calculated based on the optimum scaling factor and the quality of the fit. Events are detected when the criterion crosses a threshold level. The algorithm also automatically compensates for changes in recording noise. Amplitudes of at least three times the noise standard deviation (3 σ) were accepted. mIPSCs detected by the template were individually assessed and accepted for analysis based on two criteria: (1) mIPSCs did not overlap; and (2) records displayed a stable baseline (2.5 ms) prior to the rising phase and after the decay phase of the mIPSC. Accepted mIPSCs were aligned at their onset and averaged. Peak amplitude, rise time (calculated over 10-90% of peak amplitude), and decay time constant (calculated over 20-80% of the decay phase) were calculated within the Axograph analysis software. The decay phase of both $GABA_AR$- and GlyR-mediated mIPSCs were best fit by a single decay time constant.

Quantitative analysis of AP properties In previous *in vitro* current-clamp studies, MVN neurons have been classified, as either types A, and B (Johnston et al. 1994), or A, B, and C (Serafin et al. 1991) using qualitative features of their AP shape. Type A neurons have a monotonically rising AHP, whereas type B neurons have a biphasic AHP. Figure 2 (top and middle panels) illustrates the features of APs from type A and B MVN neurons. It has been suggested that a small group of neurons displaying intermediate characteristics can be classified as type C. In our study only neurons that

could be clearly identified as either type A or B were analyzed since those displaying intermediate characteristics may have been contaminated by cesium-based internal solution (see Results). The qualitative features were further analyzed using quantitative measures (Beraneck et al. 2003) to confirm our initial classification. These quantitative methods are outlined in Figure 2 (bottom panels). For each neuron, at least ten individual action potentials collected following breakthrough were overlaid at their onset (defined as 5% of peak) and averaged to determine AP shape. The first derivative (dV/dt) of the AHP was then calculated and plotted. As Beraneck et al (2003) have shown, the first derivative's shape is markedly different in type A and B neurons. Throughout the AHP, dV/dt of type A neurons remains positive but decreases towards zero. For type B neurons, dV/dt shows a transient negativity. This difference was independent of internal solution (CsCl vs. $KMeSO_4$ – see Fig. 5) and was present at all discharge frequencies (up to 60 Hz) reported here. Since only clearly defined type A and B neurons were parsed in the initial selection, further quantitative measures, such as convexity/concavity proved unnecessary. Similar to Beraneck et al. (2003), it should be noted, that ΔdV/dt values in this study are reported as absolute differences between the maximum and minimum deflections of the AHP dV/dt,

In our initial unbiased sample (n = 29), the proportion of neurons classified as type A and B were comparable to previous *in vitro* studies, accounting for approximately 30% and 70%, respectively (Johnston et al. 1994; Serafin et al. 1991). To provide an adequate sample of type A neurons for analysis, we deliberately biased our sample towards these neurons during latter experiments.

In addition to characterizing the MVN neuron, we also measured the following AP properties. *Spike amplitude* was defined as the maximum peak voltage (mV) taken from baseline (2.5 ms before the AP peak). *AHP amplitude* was defined as the absolute difference between the minimum of the voltage trace and baseline. *Spike width* was defined as the width of the action potential at 50% of peak amplitude. *Spike rise time* was defined as the time from 10 to 90% of *spike amplitude*. In addition, *discharge rate* was also measured and, like the previous properties, was restricted to the first two seconds after breakthrough before significant changes in spike characteristics were observed.

Neuronal labeling

In some experiments 0.5% Neurobiotin (Vector Laboratories, Burlingame, CA) was included in the recording electrode solution. Neurobiotin was allowed to passively diffuse into the cell during the recording session. Subsequently, slices were fixed in 4% paraformaldehyde overnight (4^{o}C). Neurobiotin labeling was assessed using an avidin-biotinylated peroxidase procedure (ABC Kit Elite, Vector Laboratories, Burlingame, CA) with diaminobenzidine (DAB) as the chromogen. Cobalt and nickel intensification was also used in the reaction (Adams 1981). Following visualization, slices were mounted on poly-L-lysine coated slides, air-dried and counterstained with 1% Cresyl violet. They were then passed through an ascending series of ethanols (70%, 95%, 2 x 100%), cleared in xylene, and cover-slipped in Permount (Fisher Scientific, NJ).

Labeled neurons were examined under bright field illumination, and the location of their cell bodies within the MVN was drawn on an outline of the brainstem slice using

a drawing tube attached to a microscope (Zeiss Axioskop). Since the shape of the brainstem changes significantly throughout the rostro-caudal extent of the MVN, a set of four templates (≈ 300 μm apart) from The Mouse Brain (Paxinos and Franklin 2001) were used to map the locations of labeled MVN neurons (see Fig. 7). Using the seventh cranial nerve as a landmark to determine the most rostral section, subsequent slices were sequentially assigned to the four, rostral to caudal templates. To correct for any distortion due to processing, the outline of the cut slice was scaled to match the template. The scaling factors used were then applied to the labeled neuron's dorso-ventral and medio-lateral position within the slice to calculate its normalized location within the template.

For analysis of neuron morphology each cell was drawn at high magnification (1000X). Soma area was taken as the area enclosed by a smooth line that closely followed the soma's border but excluded emerging dendritic processes (Callister et al. 1996). Soma area and maximal diameter were calculated using an image analysis package (Bioquant Image analysis Corporation, Nashville, TN). In all cases an attempt was made to follow the axon trajectory within the slice. Invariably, axons were followed to one of the cut surfaces, and therefore could not be traced to their target. For similar reasons, the complete dendritic branching pattern could not be determined.

Statistical analysis

ANOVA or t-tests were used for comparisons between variables used to assess mIPSC characteristics and action potential properties. All data are presented as means ± standard error of the mean (SEM). When analyzing the frequency distribution of

GABA only, glycine only, and Mixed mIPSCs in type A and B neurons we used a Williams' corrected 3 x 2 G-Test of independence (Sokal and Rohlf 1981). Statistical significance was set at $P < 0.05$.

RESULTS

To investigate the contribution of $GABA_A$R- and GlyR-mediated inhibitory inputs on MVN neurons, we made whole-cell patch-clamp recordings in both current- and voltage-clamp configurations from mouse brainstem slices. Recordings were made from 96 MVN neurons in the presence of CNQX (10 μM) and TTX (1 μM). In 81 of these neurons we could record clearly resolvable mIPSCs at a holding potential of –70 mV. We examined the contribution of $GABA_A$- and glycine-mediated synaptic transmission in neurons that were classified as either type A or B (n = 52). A subset of MVN neurons were also labeled with 0.5% Neurobiotin to determine whether there were morphological differences between MVN neurons based on their inhibitory profiles (n = 15) or action potential properties (n = 29).

Inhibitory profiles of MVN neurons

To determine whether mIPSCs were mediated by $GABA_A$, glycine, or both types of inhibitory receptor, we added bicuculline (10 μM), a selective antagonist for $GABA_A$Rs, to the bath. In some neurons the addition of bicuculline abolished all synaptic activity. Such neurons were classified as expressing exclusively $GABA_A$Rs (Fig. 3A). In other neurons the addition of bicuculline had no effect on mIPSC frequency, and the subsequent addition of strychnine (1 μM), a selective antagonist of GlyRs, abolished all mIPSCs. Such neurons were classified as expressing GlyRs exclusively (Fig. 3B). Finally, in some neurons addition of bicuculline decreased the frequency of mIPSCs, indicating that some, but not all, mIPSCs were $GABA_A$R-mediated (Fig. 3C). Subsequent addition of strychnine abolished the remaining synaptic activity indicating that the mIPSCs were GlyR-mediated. Such neurons were classified as expressing both $GABA_A$ and glycine receptors. Using this approach we

could establish an inhibitory profile for each recorded MVN neuron; cells were classified as receiving either exclusively $GABA_A$ergic-, exclusively glycinergic- or a mixture of $GABA_A$ergic and glycinergic mIPSCs (hereafter termed 'Mixed'). From the sample of 81 MVN neurons receiving resolvable mIPSCs, 69% (56/81) received inhibitory inputs mediated exclusively by $GABA_A$Rs (Fig. 3A). Six percent (5/81) received inhibitory inputs mediated exclusively by GlyRs (Fig 3B) and 25% (20/81) received Mixed inhibitory inputs (Fig. 3C). Whether $GABA_A$R and GlyRs are clustered underneath the same release site and activated by the co-release of both amino acid transmitters (Jonas et al. 1998), was not addressed in this study.

The properties of $GABA_A$R- and GlyR-mediated mIPSCs recorded from MVN neurons are compared in Table 1 and Figure 4. Neither input, nor series resistances were significantly different in MVN neurons used in our analysis of $GABA_A$ and GlyR- mediated mIPSC properties. Thus, any differences in mIPSC properties are not attributable to differences in intrinsic membrane properties or recording conditions. $GABA_A$R- and GlyR-mediated mIPSCs showed significant differences in several mIPSC properties. $GABA_A$R-mediated mIPSC amplitudes were smaller than those for GlyR-mediated mIPSCs (22.6 ± 1.8 *vs*. 35.3 ± 5.3 pA). The kinetics of the two receptors differed significantly, with $GABA_A$R-mediated mIPSCs having slower rise (1.3 ± 0.1 *vs.* 0.9 ± 0.1 ms) and decay times (10.5 ± 0.3 *vs*. 4.7 ± 0.3). The frequency of each type of mIPSC varied widely between neurons (0.2 – 9.0 and 0.15 – 2.5 Hz for $GABA_A$R- and GlyR-mediated events, respectively); however mean rates were not significantly different for the two types of events (1.1 ± 0.2 *vs.* 1.0 ± 0.5).

Quantitative classification of MVN neurons based on AHP properties

A principal aim of this study was to compare the contribution of $GABA_A$- and glycine-receptor mediated inhibition in the two major types of MVN neuron observed in *in vitro* recordings. Our approach was to use a CsCl-based internal solution in our recording pipette and to determine MVN type, using methods described by Beraneck and co-workers (2003), and then assess mIPSC characteristics in the **same** neuron. These experiments depend on characterizing action potential AHP features before they have been markedly altered by the accumulation of cesium ions in the recorded neuron. Thus, we performed a series of experiments where we compared the effect of Cs ions on maximum ΔdV/dt values over a 7 s period after achieving the whole-cell recording configuration with either a $KMeSO_4$- or CsCl- filled pipette. These data are compared in Figure 5. Using a $KMeSO_4$ internal (n = 5) the maximum ΔdV/dt values are not altered within 7 s of breakthrough. In contrast, in recordings made with CsCl-filled pipettes (n = 52), ΔdV/dt values decrease exponentially towards zero over the same initial 7 s period. However, ΔdV/dt values recorded within the first two seconds (epochs 1 and 2) are similar to those recorded in $KMeSO_4$ internal (left of dashed lines in Fig. 5B). Using this approach we were able to reliably distinguish type A and B MVN neurons recorded with a CsCl internal as long as the analysis was restricted to the first 2 s after breakthrough. This time is significantly shorter than the 30 – 45 seconds reported in Hefti and Smith (2003), where CsCl-based internal solution was used to classify cortical neurons based on the number of spikes fired, a characteristic much less sensitive to the effects of internal cesium.

Based on the above criteria, twenty MVN neurons were classified as type A. They displayed a single component AHP, an A-like rectification (see Beraneck et al. 2003;

Hille 2001) for description of A-like current), and dV/dt remained positive (Fig. 2A). Thirty-two MVN neurons were classed as type B neurons as they displayed a biphasic AHP and dV/dt showed a transient negativity (Fig. 2B). Eight neurons could not be confidently classified as either type A or B based on the criteria described above. Other studies (Beraneck et al. 2003; Gallagher et al. 1985; Serafin et al. 1991) have also described MVN neurons that do not fit clearly into either the type A or B class and are sometimes referred to as type C (Beraneck et al. 2003; Serafin et al. 1991). As described above, neurons that could not be confidently classified as either type A or type B were not included in this study of MVN neuron firing properties.

We also measured several AP properties in type A and B MVN neurons and these are shown in Table 2. The action potential width for type A and B neurons was not statistically different (2.2 ± 0.2 *vs*. 2.1 ± 0.1 ms, respectively), and neither was spike amplitude (63.7 ± 2.7 *vs*. 71.0 ± 2.4 mV). In contrast, AHP amplitude (16.9 ± 1.3 *vs*. 13.8 ± 0.8 mV; $P < 0.05$) differed significantly in type A versus B MVN neurons, respectively. The discharge rate of type A neurons was also significantly higher than for type B neurons (29.7 ± 4.0 *vs.* 14.3 ± 1.3 Hz; $P < 0.001$).

Inhibitory profiles of type A and B MVN neurons

Since MVN neurons can be classified according to the shape of their AHP, **and** the type of inhibitory inputs they receive, we determined whether there was a differential distribution of inhibitory inputs onto type A and B MVN neurons. In 52 MVN neurons that could be confidently assigned as type A or B (see above) we were able to determine their inhibitory profiles (Fig. 6). Type A MVN neurons were dominated by exclusively $GABA_A$ergic mIPSCs (n = 15 of 20) with only a single neuron showing both $GABA_A$ergic and glycinergic (Mixed) inhibition. The remaining type A neurons

(n = 4) had no detectable mIPSCs. Type B neurons also displayed exclusively $GABA_A$ergic mIPSCs (n = 15), however significantly more neurons received glycinergic input, some receiving exclusively glycinergic mIPSCs (n = 2) as well as Mixed inputs (n = 10). The remaining type B neurons (n = 5) had no detectable mIPSCs. The difference in inhibitory profiles of type A and B neurons was statistically significant ($G_{STAT} = 7.28$, df = 2; $p < 0.05$).

Morphological characteristics of MVN neurons

A subset of MVN neurons were labeled with 0.5% Neurobiotin to determine whether there were location, and/or morphological differences between MVN neurons based on either action potential properties, or inhibitory profiles (Table 3, and Fig. 7). In 29 neurons, 7 were classified as type A and 22 were classified as type B (Table 3). Soma area and maximal soma diameter were similar in type A and B MVN neurons (179.2 ± 27.8 *vs.* 162.1 ± 15.9 μm^2 and 21.4 ± 2.2 *vs.* 18.6 ± 1.6 μm, respectively). Similarly, no differences were observed in the number of primary dendrites (4.0 ± 0.5 *vs*. 3.9 ± 0.3). The morphological features of MVN neurons were also compared in cells with different inhibitory profiles. A sample of fifteen neurons was classified in this manner. Of these neurons, 10 received exclusively $GABA_A$ergic inhibitory inputs, 1 received exclusively glycinergic inputs and 4 received mixed inhibitory inputs. Soma area, maximum soma diameter and number of primary dendrites were similar in neurons receiving exclusively $GABA_A$ergic-, exclusively glycinergic-, or both types of mIPSCs (Table 3). Taken together, these data suggest that neuron morphology is not associated with either its discharge characteristics or the type of inhibitory inputs it receives. Morphological characteristics were also not helpful distinguishing MVN neuron discharge properties in rat (Sekirnjak and du Lac, 2002).

DISCUSSION

Inhibitory inputs to MVN neurons

Prior to this report, only one study has recorded mIPSCs and characterized the nature of spontaneous inhibitory synaptic transmission on MVN neurons in a mammal. These experiments used young rats (P13-17) and showed that spontaneous IPSCs were mediated exclusively by $GABA_A$Rs (Chun et al. 2003). Since eye opening in rats and mice occurs at approximately P12-13 (Henneberger et al. 2005; Zhang et al. 2005), and MVN neurons in both species display electrophysiological properties similar to those in adult animals after P15 (Murphy and Du Lac 2001), it is possible that the lack of glycine receptors reflects an earlier developmental synaptic profile of MVN neurons (for review see Straka et al. 2005). Inhibitory postsynaptic events have been recorded from embryonic (E16) and neonatal (1-day-old hatchlings) second-order vestibular neurons in the chick tangential nucleus (Shao et al. 2004, 2003). Although a non-mammalian species, these studies showed the presence of both receptors and a significant developmental shift in the contribution of $GABA_A$R-mediated (74% to 44%) and GlyR-mediated (26% to 56%) spontaneous IPSCs. Our data in mouse brainstem slices show that for MVN neurons displaying resolvable mIPSCs, almost all (94% = 69% $GABA_A$ergic only + 25% Mixed) received $GABA_A$R-mediated inhibitory inputs. In contrast, only 31% receive GlyR-mediated inhibitory inputs, (6% glycinergic only and 25% Mixed).

Our data are consistent with numerous studies that have provided evidence for $GABA_A$- and/or GlyR expression in the postsynaptic membranes of MVN neurons in a number of species. Physiological studies have been largely based on the affects of applied agonists or antagonists on the spontaneous discharge rate of MVN neurons.

(Dutia et al. 1992; Lapeyre and De Waele 1995; Precht et al. 1973; Vibert et al. 2000). Anatomical studies have also provided evidence for the presence of $GABA_A$- and GlyRs in the MVN (for review see de Waele et al. 1995). More recently, exhaustive analyses using *in situ* hybridization (Pirker et al. 2000) together with immunofluorescence (Eleore et al. 2005; Eleore et al. 2004; Horii et al. 2004) have described the presence of various $GABA_AR$ and GlyR subunits in rat MVN neurons. However, these studies only reveal the presence or absence of a particular receptor, and they do not distinguish between receptors located under a functional synapse, or those located extra-synaptically. Our study shows $GABA_A$- mediated **synaptic** inhibition dominates in the mouse MVN, although the contribution of GlyRs is significant.

$GABA_AR$-mediated mIPSCs in mouse MVN neurons displayed smaller amplitudes and slower kinetics (rise times and decay times) than GlyR-mediated mIPSCs. These results are similar to those reported for other rodent CNS regions where $GABA_A$ and GlyR mediated mIPSCs have been compared (Donato and Nistri 2000; Graham et al. 2003; Nabekura et al. 2004; O'Brien and Berger 2001; O'Brien et al. 2004; Russier et al. 2002). Furthermore, the kinetics for $GABA_A$-mediated and GlyR-mediated mIPSCs are similar to those recorded in other brainstem nuclei under similar conditions (Callister et al. 1999; O'Brien and Berger 2001). When combined with recent *in situ* hybridization and protein expression studies some insight into the subunit composition of the relevant receptors in mouse MVN can be gained. The available data in rat suggests MVN $GABA_ARs$ are composed of $\alpha1$, $\beta2$ /3, and $\gamma2$ subunits, while GlyRs are composed of $\alpha1$, and β subunits (Eleore et al. 2005; Eleore et al. 2004; O'Brien and Berger 2001). As both $GABA_ARs$ and GlyRs in mice have

similar kinetics to those in rats, we would predict similar subunit compositions in the mouse MVN (O'Brien and Berger, 2001; Singer et al. 1998).

While our results show that both $GABA_A$- and GlyRs are clustered under release sites and contribute to fast inhibitory synaptic transmission in mouse MVN neurons, the exact origin of these inhibitory inputs is unclear. Previous studies have demonstrated that $GABA_A$-mediated inhibitory inputs onto MVN neurons come from at least two sources: the cerebellum, via GABA-releasing Purkinje cells (Babalian and Vidal 2000; Cox and Peusner 1990; du Lac and Lisberger 1992), and from contralateral MVN neurons via commissural connections between the MVN on either side of the brainstem (Furuya et al. 1991; Shimazu and Precht 1966). The origin of glycinergic inhibitory inputs to MVN neurons is less clear. Some authors suggest that GlyR-mediated inhibitory inputs arise from contralateral MVN neurons and project across the midline via the commissural pathway (Precht et al. 1973), whereas others suggest that these inputs arise from ipsilateral local circuit MVN interneurons (Furuya et al. 1991; Shimazu and Precht 1966).

Classification of MVN neurons

Previous studies have classified MVN neurons into types A, B or C (Beraneck et al. 2003; Gallagher et al. 1985; Johnston et al. 1994; Serafin et al. 1991) based on the shape of the action potential's AHP. It is accepted, however, that MVN neurons probably form a continuum between canonical type A and B neurons (Beraneck et al. 2003; du Lac and Lisberger 1995). In the present study, we classified neurons as either type A or B. Early studies (Johnston et al. 1994; Serafin et al. 1991) report broader spike width, and slower rise times for type A neurons. In our study no

significant differences were observed in AP characteristics such as spike width, and rise time, for type A and B MVN neurons. This could be attributed to our recordings using patch electrodes with a CsCl-based internal solution at room temperature, Indeed, increased background discharge rates are consistent with the known inhibitory effect of cesium on potassium channels responsible for action potential repolarization (Hille 2001). A more recent study (Beraneck et al. 2003) however, concludes that spike width and rise time are not sufficient to distinguish the two types of MVN neurons.

Inhibitory drive in type A and B MVN neurons

The major goal of this study was to compare the nature of fast inhibitory synaptic drive in type A and B MVN neurons. We used a CsCl-based internal solution and recorded spontaneous action potentials **immediately** after (Hefti and Smith 2003) achieving the whole-cell current clamp configuration (see Figs. 1 & 5). This approach allowed classification of neurons based on their AP properties (see Fig. 2), and subsequent voltage-clamp recording of low noise mIPSCs at near resting membrane potential (-70 mV). Moreover, recordings made under these conditions can be readily compared to the large rodent literature on $GABA_A$- and GlyR-mediated mIPSC properties (see Table 1) in other CNS regions (Graham et al. 2003; Legendre 2001; O'Brien et al. 2004).

Our results show that $GABA_A$R-mediated inhibitory drive is directed to *both* type A and B MVN neurons. In contrast, GlyR-mediated inhibitory drive is confined almost exclusively to type B neurons. Our data are based on the observation that glycinergic mIPSCs are absent in type A neurons during the three minutes following bicuculline

block. This, however, may not reflect a total lack of GlyRs. For instance, small glycinergic events may be obscured at room temperature due to their low frequency and reduced kinetics. However, since all neurons, regardless of type, were exposed to the same conditions, this strongly argues that the results reflect a fundamental difference in the inhibitory profiles of type A and B neurons. It is also possible that glycinergic receptors are located on distal dendrites of type A neurons and thus, in some cases, were removed during tissue processing. Again, this still represents a significant asymmetry in glycinergic synaptic transmission between type A and type B neurons.

The functional significance of these findings are open to interpretation. Given the differences in amplitude and time course of $GABA_A$ and GlyR-mediated mIPSCs (Table 1), the characteristics of the hyperpolarization produced by activation of either receptor would be markedly different. For example, the longer decay time of $GABA_A$R-mediated input would provide prolonged hyperpolarization, shunting of excitatory events, and decreased MVN neuron discharge to both type A and B neurons. In contrast, activation of GlyRs, available almost exclusively to type B neurons, would allow additional brief blockade of MVN neuron discharge.

To understand the implication of our results, precise information regarding the *in vivo* function of type A and B MVN neurons is needed. Previously, *in vivo* MVN neurons have been classified according to their responses to ipsilateral head rotation (type I and type II, and in some cases type III; (Duensing and Schaefer 1958; Precht and Shimazu 1965; Shimazu and Precht 1965). Type I neurons have been further subdivided into *tonic* and *kinetic*, based on the regularity of their background

discharge pattern (Shimazu and Precht 1965). Indirect attempts to consolidate *in vivo* and *in vitro* schemes (I and II vs. A and B) have been made and suggest that type A MVN neurons (*in vitro*) correspond with type I tonic neurons (*in vivo*), and type B neurons correspond with type I kinetic neurons (Babalian et al. 1997; Vidal et al. 1996). Thus it is possible that type A (type I tonic) neurons are modulated almost exclusively by $GABA_AR$-mediated inputs, whereas type B (type I kinetic) neurons may be modulated by exclusively $GABA_AR$-mediated inputs, exclusively GlyR-mediated inputs, or a combination of both. The differential distribution of inhibitory inputs onto type A and B MVN neurons observed in this study would therefore confer distinct physiological functions for tonic and kinetic neurons recorded *in vivo*.

A recent study has implied an alternative relationship. It is reported that neurons displaying properties *similar* to type A are 'interneurons' (as suggested by Takazawa et al. 2004) and by inference, equivalent to *in vivo* type II, and not type I, neurons. If correct, this suggests that type II neurons receive predominately $GABA_A$ergic inputs. In addition, Takazawa et al., showed that glutamatergic neurons always display type B characteristics whereas GABAergic neurons were more heterogenous. Therefore another possibility is that glutaminergic neurons receive glycinergic input whereas GABAergic neurons may not. The resolution of these issues awaits further study.

Conclusion

This study represents the first electrophysiological investigation of inhibitory synaptic input onto physiologically classified type A and B MVN neurons. Our data demonstrate a clear differential distribution of inhibitory inputs onto type A and B MVN neurons. Type A neurons receive almost exclusively $GABA_A$ergic inhibitory

inputs, while type B neurons can receive a significant additional glycinergic input. Although these data provide potential evidence for discrete roles for $GABA_A$ergic and glycinergic synaptic transmission in type A and B MVN neurons, it is not possible at this stage to confidently state what this means for MVN neurons *in vivo*. The technically challenging *in vivo* patch-clamp recording technique, as recently applied to spinal and cortical neurons (Brecht et al. 2004; Graham et al. 2004), could be applied to MVN neurons to address this issue. Using this approach it would be possible to examine subthreshold events associated with a neuron's response to both natural stimulation (e.g. head rotation), and current injection. Such experiments would therefore allow the precise role of inhibitory synaptic transmission in functioning vestibular-mediated pathways to be determined.

Acknowledgements

Thanks to Melissa Walsh and Sally Hilton for assistance with the processing of labeled neurons and production of Figure 7, and Elizabeth Lamont for proofreading the manuscript. We also thank the National Health and Medical Research Council of Australia, The Garnett Passe and Rodney Williams Foundation, and Hunter Medical Research Institute for support.

REFERENCES

Adams JC. Heavy metal intensification of DAB-based HRP reaction product. *J Histochem Cytochem* 29: 775, 1981.

Babalian A, Vibert N, Assie G, Serafin M, Muhlethaler M, and Vidal PP. Central vestibular networks in the guinea-pig: functional characterization in the isolated whole brain in vitro. *Neuroscience* 81: 405-426, 1997.

Babalian AL and Vidal PP. Floccular modulation of vestibuloocular pathways and cerebellum-related plasticity: An in vitro whole brain study. *J Neurophysiol* 84: 2514-2528, 2000.

Barmack NH. Central vestibular system: vestibular nuclei and posterior cerebellum. *Brain Res Bull* 60: 511-541, 2003.

Beraneck M, Hachemaoui M, Idoux E, Ris L, Uno A, Godaux E, Vidal PP, Moore LE, and Vibert N. Long-term plasticity of ipsilesional medial vestibular nucleus neurons after unilateral labyrinthectomy. *J Neurophysiol* 90: 184-203, 2003.

Brecht M, Schneider M, Sakmann B, and Margrie TW. Whisker movements evoked by stimulation of single pyramidal cells in rat motor cortex. *Nature* 427: 704-710, 2004.

Callister RJ, Donnelly RP, Pierce PA, and Stuart DG. Motor pool organization of the external gastrocnemius muscle in the turtle, Pseudemys (Trachemys) scripta elegans. *J Morphol* 227: 171-183, 1996.

Callister RJ, Schofield PR, and Sah P. Use of murine mutants to study glycine receptor function. *Clin Exp Pharmacol Physiol* 26: 929-931, 1999.

Cameron SA and Dutia MB. Cellular basis of vestibular compensation: changes in intrinsic excitability of MVN neurones. *Neuroreport* 8: 2595-2599, 1997.

Chun SW, Choi JH, Kim MS, and Park BR. Characterization of spontaneous synaptic transmission in rat medial vestibular nucleus. *Neuroreport* 14: 1485-1488, 2003.

Clements JD and Bekkers JM. Detection of spontaneous synaptic events with an optimally scaled template. *Biophys J* 73: 220-229, 1997.

Cox RG and Peusner KD. Horseradish peroxidase labeling of the efferent and afferent pathways of the avian tangential vestibular nucleus. *J Comp Neurol* 296: 324-341, 1990.

Curthoys IS and Halmagyi GM. Vestibular compensation: a review of the oculomotor, neural, and clinical consequences of unilateral vestibular loss. *J Vestib Res* 5: 67-107, 1995.

Darlington CL and Smith PF. Molecular mechanisms of recovery from vestibular damage in mammals: recent advances. *Prog Neurobiol* 62: 313-325, 2000.

de Waele C, Muhlethaler M, and Vidal PP. Neurochemistry of the central vestibular pathways. *Brain Res Brain Res Rev* 20: 24-46, 1995.

Donato R and Nistri A. Relative contribution by GABA or glycine to Cl(-)-mediated synaptic transmission on rat hypoglossal motoneurons in vitro. *J Neurophysiol* 84: 2715-2724, 2000.

du Lac S and Lisberger SG. Eye movements and brainstem neuronal responses evoked by cerebellar and vestibular stimulation in chicks. *J Comp Physiol [A]* 171: 629-638, 1992.

du Lac S and Lisberger SG. Membrane and firing properties of avian medial vestibular nucleus neurons in vitro. *J Comp Physiol [A]* 176: 641-651, 1995.

Duensing F and Schaefer KP. [The activity of single neurons in the region of vestibular nuclei in horizontal acceleration, with special reference to vestibular nystagmus.]. *Arch Psychiatr Nervenkr Z Gesamte Neurol Psychiatr* 198: 225-252, 1958.

Dutia MB, Johnston AR, and McQueen DS. Tonic activity of rat medial vestibular nucleus neurones in vitro and its inhibition by GABA. *Exp Brain Res* 88: 466-472, 1992.

Dutia MB and Johnston AR Development of action potentials and apamin-sensitive after-potentials in mouse vestibular nucleus neurones. *Exp Brain Res* 118: 148-154, 1998.

Eleore L, Vassias I, Bernat I, Vidal PP, and de Waele C. An in situ hybridization and immunofluorescence study of GABA(A) and GABA(B) receptors in the vestibular nuclei of the intact and unilaterally labyrinthectomized rat. *Exp Brain Res* 160: 166-179, 2005.

Eleore L, Vassias I, Vidal PP, and de Waele C. An in situ hybridization and immunofluorescence study of glycinergic receptors and gephyrin in the vestibular nuclei of the intact and unilaterally labyrinthectomized rat. *Exp Brain Res* 154: 333-344, 2004.

Furuya N, Yabe T, and Koizumi T. Neurotransmitters regulating vestibular commissural inhibition in the cat. *Acta Otolaryngol Suppl* 481: 205-208, 1991.

Gallagher JP, Lewis MR, and Gallagher PS. An electrophysiological investigation of the rat medial vestibular nucleus in vitro. *Prog Clin Biol Res* 176: 293-304, 1985.

Goldberg JM. Afferent diversity and the organization of central vestibular pathways. *Exp Brain Res* 130: 277-297, 2000.

Graham BA, Brichta AM, and Callister RJ. In vivo responses of mouse superficial dorsal horn neurones to both current injection and peripheral cutaneous stimulation. *J Physiol* 561: 749-763, 2004.

Graham BA, Schofield PR, Sah P, and Callister RJ. Altered inhibitory synaptic transmission in superficial dorsal horn neurones in spastic and oscillator mice. *J Physiol* 551: 905-916, 2003.

Hefti BJ and Smith PH. Distribution and kinetic properties of GABAergic inputs to layer V pyramidal cells in rat auditory cortex. *J Assoc Res Otolaryngol* 4: 106-121, 2003.

Henneberger C, Juttner R, Schmidt SA, Walter J, Meier JC, Rothe T, and Grantyn R. GluR- and TrkB-mediated maturation of GABA receptor function during the period of eye opening. *Eur J Neurosci* 21: 431-440, 2005.

Hille B. *Ion channels of excitable membranes*. Massachusetts: Sinauer associates inc., 2001.

Horii A, Masumura C, Smith PF, Darlington CL, Kitahara T, Uno A, Mitani K, and Kubo T. Microarray analysis of gene expression in the rat vestibular nucleus complex following unilateral vestibular deafferentation. *J Neurochem* 91: 975-982, 2004.

Johnston AR, Him A, and Dutia MB. Differential regulation of GABA(A) and GABA(B) receptors during vestibular compensation. *Neuroreport* 12: 597-600, 2001.

Johnston AR, MacLeod NK, and Dutia MB. Ionic conductances contributing to spike repolarization and after-potentials in rat medial vestibular nucleus neurones. *J Physiol* 481 (Pt 1): 61-77, 1994.

Jonas P, Bischofberger J, and Sandkuhler J. Corelease of two fast neurotransmitters at a central synapse. *Science* 281: 419-424, 1998.

Lapeyre PN and De Waele C. Glycinergic inhibition of spontaneously active guinea-pig medial vestibular nucleus neurons in vitro. *Neurosci Lett* 188: 155-158, 1995.

Legendre P. The glycinergic inhibitory synapse. *Cell Mol Life Sci* 58: 760-793, 2001.

Lim R, Oleskevich S, Few AP, Leao RN, and Walmsley B. Glycinergic mIPSCs in mouse and rat brainstem auditory nuclei: modulation by ruthenium red and the role of calcium stores. *J Physiol* 546: 691-699, 2003.

Murphy GJ and Du Lac S. Postnatal development of spike generation in rat medial vestibular nucleus neurons. *J Neurophysiol* 85: 1899-1906, 2001.

Nabekura J, Katsurabayashi S, Kakazu Y, Shibata S, Matsubara A, Jinno S, Mizoguchi Y, Sasaki A, and Ishibashi H. Developmental switch from GABA to glycine release in single central synaptic terminals. *Nat Neurosci* 7: 17-23, 2004.

O'Brien JA and Berger AJ. The nonuniform distribution of the GABA(A) receptor alpha 1 subunit influences inhibitory synaptic transmission to motoneurons within a motor nucleus. *J Neurosci* 21: 8482-8494, 2001.

O'Brien JA, Sebe JY, and Berger AJ. GABA(B) modulation of GABA(A) and glycine receptor-mediated synaptic currents in hypoglossal motoneurons. *Respir Physiol Neurobiol* 141: 35-45, 2004.

Paxinos G and Franklin KBJ. *The Mouse Brain in Stereotaxic Coordinates*. San Diego: Academic Press, 2001.

Pirker S, Schwarzer C, Wieselthaler A, Sieghart W, and Sperk G. GABA(A) receptors: immunocytochemical distribution of 13 subunits in the adult rat brain. *Neuroscience* 101: 815-850, 2000.

Precht W, Schwindt PC, and Baker R. Removal of vestibular commissural inhibition by antagonists of GABA and glycine. *Brain Res* 62: 222-226, 1973.

Precht W and Shimazu H. Functional connections of tonic and kinetic vestibular neurons with primary vestibular afferents. *J Neurophysiol* 28: 1014-1028, 1965.

Russier M, Kopysova IL, Ankri N, Ferrand N, and Debanne D. GABA and glycine co-release optimizes functional inhibition in rat brainstem motoneurons in vitro. *J Physiol* 541: 123-137, 2002.

Serafin M, de Waele C, Khateb A, Vidal PP, and Muhlethaler M. Medial vestibular nucleus in the guinea-pig. I. Intrinsic membrane properties in brainstem slices. *Exp Brain Res* 84: 417-425, 1991.

Shao M, Hirsch JC, Giaume C, and Peusner KD. Spontaneous synaptic activity in chick vestibular nucleus neurons during the perinatal period. *Neuroscience* 127: 81-90, 2004.

Shao M, Hirsch JC, Giaume C, and Peusner KD. Spontaneous synaptic activity is primarily GABAergic in vestibular nucleus neurons of the chick embryo. *J Neurophysiol* 90: 1182-1192, 2003.

Shimazu H and Precht W. Inhibition of central vestibular neurons from the contralateral labyrinth and its mediating pathway. *J Neurophysiol* 29: 467-492, 1966.

Shimazu H and Precht W. Tonic and kinetic responses of cat's vestibular neurons to horizontal angular acceleration. *J Neurophysiol* 28: 991-1013, 1965.

Singer JH, Talley EM, Bayliss DA, and Berger AJ. Development of glycinergic synaptic transmission to rat brain stem motoneurons. *J Neurophysiol* 80: 2608-2620, 1998.

Sekirnjak C and du Lac S. Intrinsic firing dynamics of vestibular nucleus neurons. *J Neurosci* 22: 2083-2095, 2002.

Smith PF and Curthoys IS. Mechanisms of recovery following unilateral labyrinthectomy: a review. *Brain Res Brain Res Rev* 14: 155-180, 1989.

Sokal RR and Rohlf FJ. *Biometry*. San Francisco: W.H. Freeman and Co., 1981.

Spencer RF and Baker R. GABA and glycine as inhibitory neurotransmitters in the vestibuloocular reflex. *Ann N Y Acad Sci* 656: 602-611, 1992.

Straka H and Dieringer N. Uncrossed disynaptic inhibition of second-order vestibular neurons and its interaction with monosynaptic excitation from vestibular nerve afferent fibers in the frog. *J Neurophysiol* 76: 3087-3101, 1996.

Straka H, Vibert N, Vidal PP, Moore LE, and Dutia MB. Intrinsic membrane properties of vertebrate vestibular neurons: Function, development and plasticity. *Prog Neurobiol*, 2005.

Takazawa T, Saito Y, Tsuzuki K, and Ozawa S. Membrane and firing properties of glutamatergic and GABAergic neurons in the rat medial vestibular nucleus. *J Neurophysiol*, 2004.

Vibert N, Beraneck M, Bantikyan A, and Vidal PP. Vestibular compensation modifies the sensitivity of vestibular neurones to inhibitory amino acids. *Neuroreport* 11: 1921-1927, 2000.

Vidal PP, Babalian A, Vibert N, Serafin M, and Muhlethaler M. In vivo-in vitro correlations in the central vestibular system: a bridge too far? *Ann N Y Acad Sci* 781: 424-436, 1996.

Wilson VJ and Melvill Jones G. *Mammalian Vestibular Physiology*. New York: Plenum Press, 1979.

Yamanaka T, Him A, Cameron SA, and Dutia MB. Rapid compensatory changes in GABA receptor efficacy in rat vestibular neurones after unilateral labyrinthectomy. *J Physiol* 523 Pt 2: 413-424, 2000.

Zhang J, Yang Z, and Wu SM. Development of cholinergic amacrine cells is visual activity-dependent in the postnatal mouse retina. *J Comp Neurol* 484: 331-343, 2005.

Figure 1. Experimental protocol

Using a CsCl-based internal electrode solution, action potentials and mIPSCs were recorded from the same MVN neuron. *A*. Examples of recording configurations used during the experimental protocol. (*1*) Occasional extracellular activity was recorded in cell-attached current-clamp mode. (*2*) Following breakthrough, action potentials were recorded in whole-cell current-clamp. (*3*) The recording configuration was then changed to whole-cell voltage-clamp mode to record mIPSCs. *B*. A continuous recording from a MVN neuron showing the experimental protocol. Action potentials were recorded in whole-cell current-clamp immediately following membrane breakthrough (arrow). Note that action potential amplitude decreases with time, and the gradual depolarization of the baseline. These effects were attributed to CsCl loading of the cell interior. The transition from current-clamp (CC) to voltage-clamp (VC) is indicated by I = 0. mIPSCs were recorded in whole-cell voltage-clamp at a holding potential of –70 mV.

Figure 2. Classification of MVN neurons

Spontaneous action potentials recorded immediately after breakthrough (during the first two seconds) with a CsCl-based internal electrode solution were used to classify MVN neurons based on AHP characteristics. *A* and *B* (top traces), action potentials recorded following membrane breakthrough from a type A MVN neuron, and type B MVN neuron, respectively. *A* (middle trace), action potential AHP on expanded time scale recorded in a type A MVN neuron displaying characteristic AHP concavity and A-like rectification *(arrowhead)*. *B* (middle trace), Action potential AHP recorded from a type B MVN neuron displaying an early fast (*asterisk)*, and a late slow convex AHP component *(arrow)*. *A* and *B* (bottom traces), the first derivative (dV/dt) of the average AHP profile of a type A (mean of 55 spikes) and type B (mean of 38 spikes) MVN neuron, respectively. Note that the first derivative remains above the zero line (positive) in type A MVN neurons, while type B MVN neurons display a period of negativity (arrows) following the brief positive peak.

Figure 3. Identification and classification of inhibitory profiles in MVN neurons

Experiments *A*-*C* show mIPSCs recorded at a holding potential of –70 mV from three MVN neurons with different inhibitory profiles. *A*, The upper trace shows mIPSCs recorded in the presence of CNQX (10 μM) and TTX (1 μM). Adding bicuculline (10 μM) to the bath (lower trace) abolished all synaptic activity, confirming that mIPSCs isolated in the upper trace were exclusively $GABA_A$R-mediated. *B*, In a different neuron, mIPSCs isolated in CNQX and TTX (upper trace) were unaffected by addition of bicuculline (middle trace), however subsequent addition of strychnine (1 μM) to the bath abolished all synaptic activity (lower trace), confirming that mIPSCs isolated in CNQX, TTX, and bicuculline were GlyR-mediated. *C*, Other neurons received a combination of $GABA_A$R- and GlyR-mediated mIPSCs. In these neurons, addition of bicuculline (middle trace) reduced mIPSC amplitude and frequency. All remaining synaptic activity was abolished by addition of strychnine (lower trace). Asterisks denote 10 mV voltage step used to monitor series and input resistance during mIPSC recording.

Figure 4. mIPSC properties

A, Comparison of $GABA_AR$-mediated mIPSCs (top trace) and GlyR-mediated mIPSCs (bottom trace). Note, glycinergic mIPSCs have large amplitudes and faster kinetics. *B*. Averaged $GABA_AR$ - and GlyR-mediated mIPSCs isolated from recordings shown in *A* (average of 225 and 221 records respectively). Overlapping traces (bottom) show averaged mIPSCs normalized to the same amplitude. Note that $GABA_AR$-mediated mIPSCs have slower decay times than GlyR-mediated mIPSCs. *C*. Bar graphs comparing $GABA_AR$ - and GlyR-mediated mIPSC amplitude, rise time, decay, and frequency. Asterisks indicate significant difference in mIPSC properties. Values within bars indicate the number of cells sampled.

Figure 5. Comparison of ΔdV/dt values recorded with $KMeSO_4$ and CsCl internal pipette solutions

We recorded APs over a 7 second period following membrane breakthrough using $KMeSO_4$ (left) or CsCl (right) based internal solutions. *A.* Continuous record from a type B MVN neuron obtained with a CsCl based internal solution (truncated at 4 seconds). For subsequent analysis of the AHP, APs recorded immediately following membrane breakthrough were captured and averaged over 1-second epochs (eg, epoch 1; 0-1 s). The average spike profile from each epoch was then used to calculate a maximum value of ΔdV/dt (as in lower panels of Fig. 2) over the 1-second interval. *B.* Comparison of type B neurons recorded in $KMeSO_4$ (left trace) and CsCl (right trace) showing little or no qualitative differences in the initial stages. *C.* Maximal ΔdV/dt value plotted over 7 seconds for five type A (upper traces) and five type B (lower two traces) MVN neurons. Data from $KMeSO_4$-based internal are shown on the left (open symbols); CsCl-based internal on the right (solid symbols). For neurons recorded using a $KMeSO_4$-based internal (n = 5), maximal ΔdV/dt values were unchanged over the 7-second interval. Data points were best fit with a straight line. For neurons recorded using a CsCl-based internal (n = 5), maximal ΔdV/dt values decreased, and the data points are best fit with a single exponential. Note, however, maximal ΔdV/dt values in the first two epochs (left of dashed lines) are similar to those recorded in $KMeSO_4$-based internal. Transient negativity values, the main distinguishing feature of type B neurons, were also plotted (bottom traces). Although values were reduced with time using a CsCl-based internal, they were comparable with those recorded in $KMeSO_4$ in the first two seconds following breakthrough. Consequently, for CsCl-based internal recordings we restricted our analysis to those APs recorded in the first 2 seconds after membrane breakthrough.

Figure 6. Inhibitory profiles of Type A and B MVN neurons

MVN neurons classified into type A and B MVN neurons show a differential distribution of inhibitory inputs. Type A MVN neurons (n=20) receive exclusively $GABA_A$ergic inhibitory inputs (GABA), sparse mixed (Mix) inputs, or no resolvable inhibitory inputs (Nil); whereas type B MVN neurons (n=32) receive, in addition to exclusively $GABA_A$ergic inputs, a significant proportion of glycinergic (Gly), and mixed inhibitory inputs.

Figure 7. Location and Morphology of characterized MVN neurons

A subset of MVN neurons was labeled with Neurobiotin to characterize both their location within the MVN, and their morphology. *A*, micrograph (right inset; scale bar = 1 mm) showing dorsal view of the isolated brainstem and location of transverse sections represented on the left.. The four transverse brainstem templates (1-4; Figures 81, 83, 86, and 88 from The Mouse Brain (Paxinos and Franklin 2001); approx. 300 μm apart) were used to plot the location of physiologically characterized MVN neurons (scale bar = 500 μm). Type A (n=7) and B (n=22) neurons (left side of template) were located throughout the rostrocaudal extent of the MVN. Plots of MVN neurons according to inhibitory profiles are shown on the right side of templates (n = 15). *B1 & B2*, photomicrographs (left) and drawing tube reconstructions (right) of a type A and type B MVN neuron. Scale bar = 20 μm. Type A and B neurons displayed similar sized somas and number of primary dendrites (see Table 3).

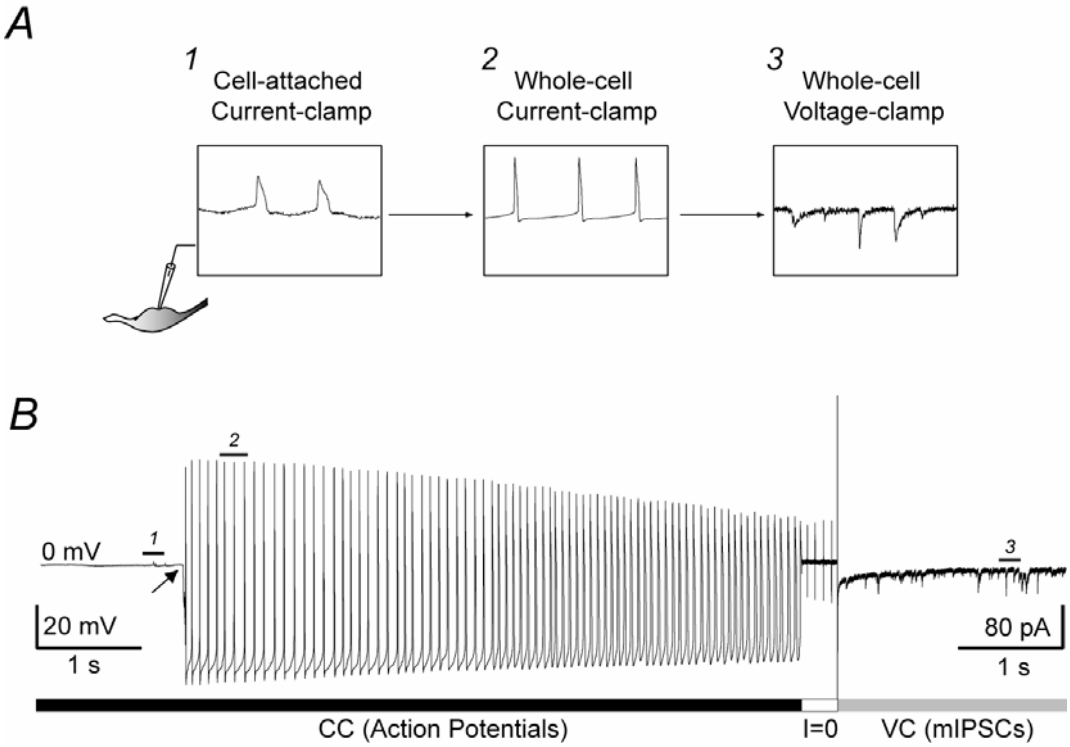

Figure 1:
Camp et al.

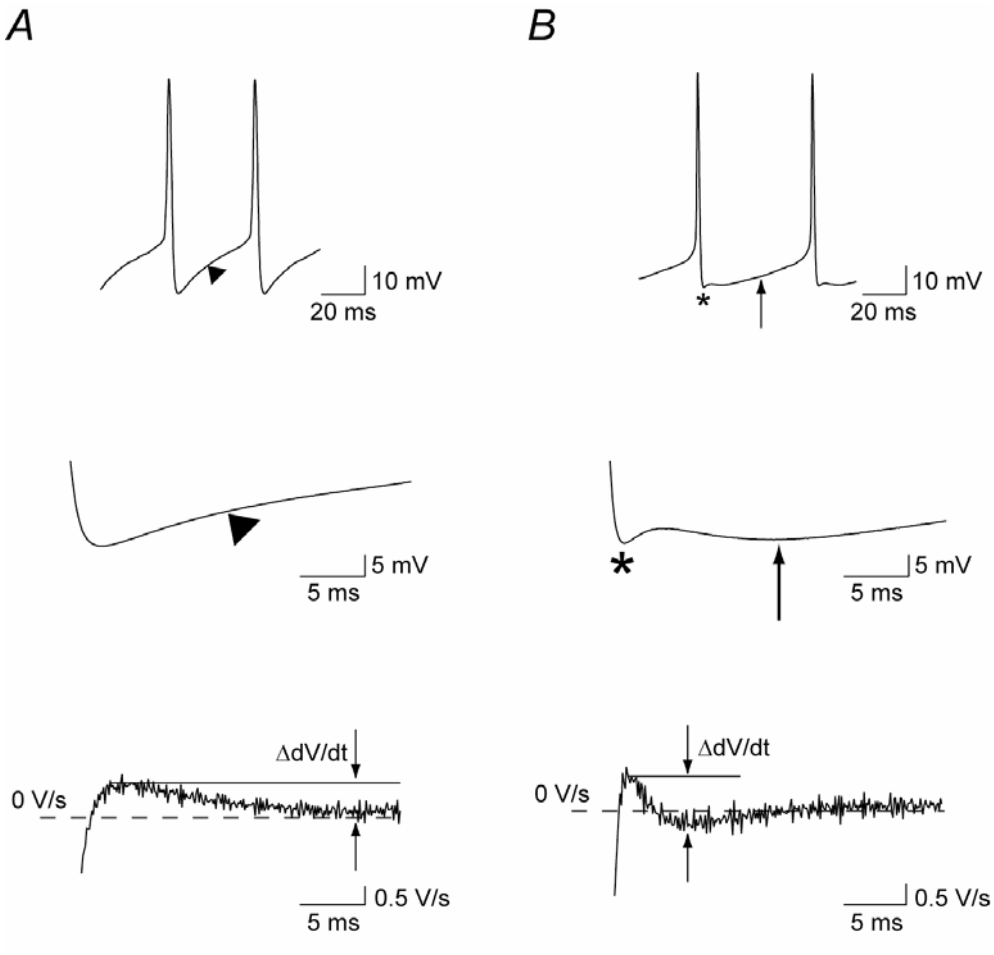

Figure 2
Camp et al.

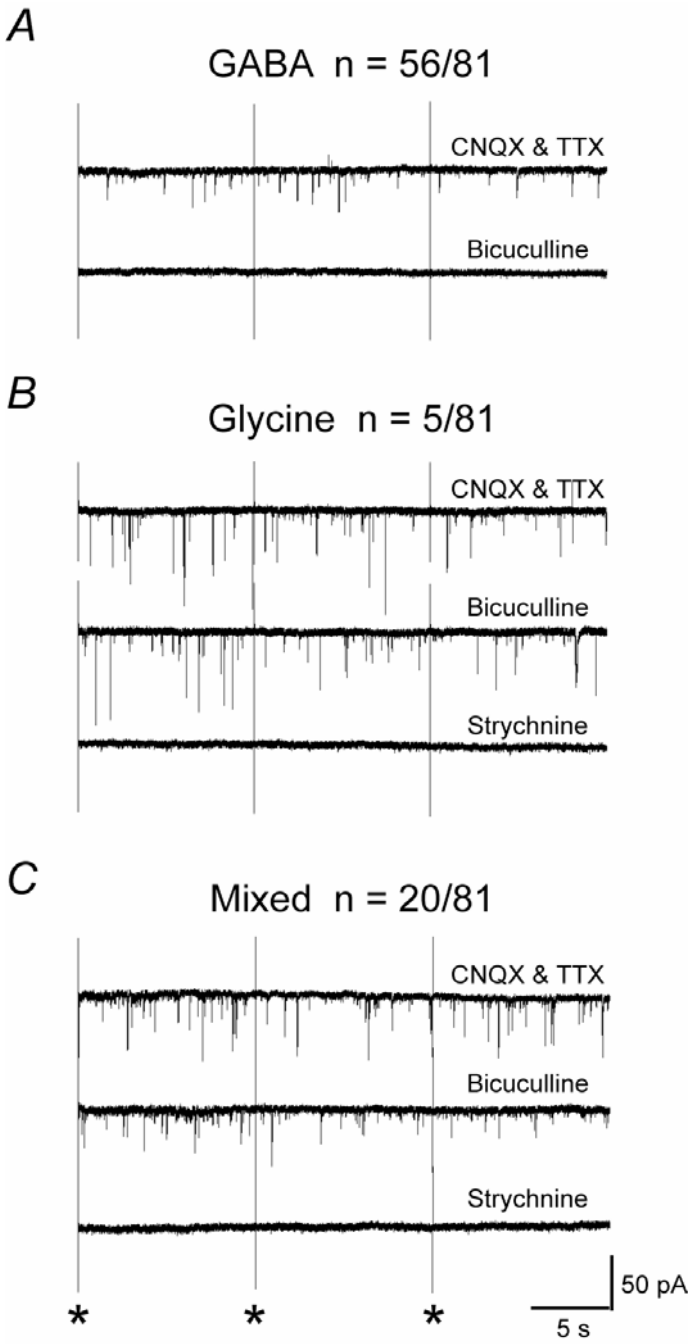

Figure 3:
Camp et al.

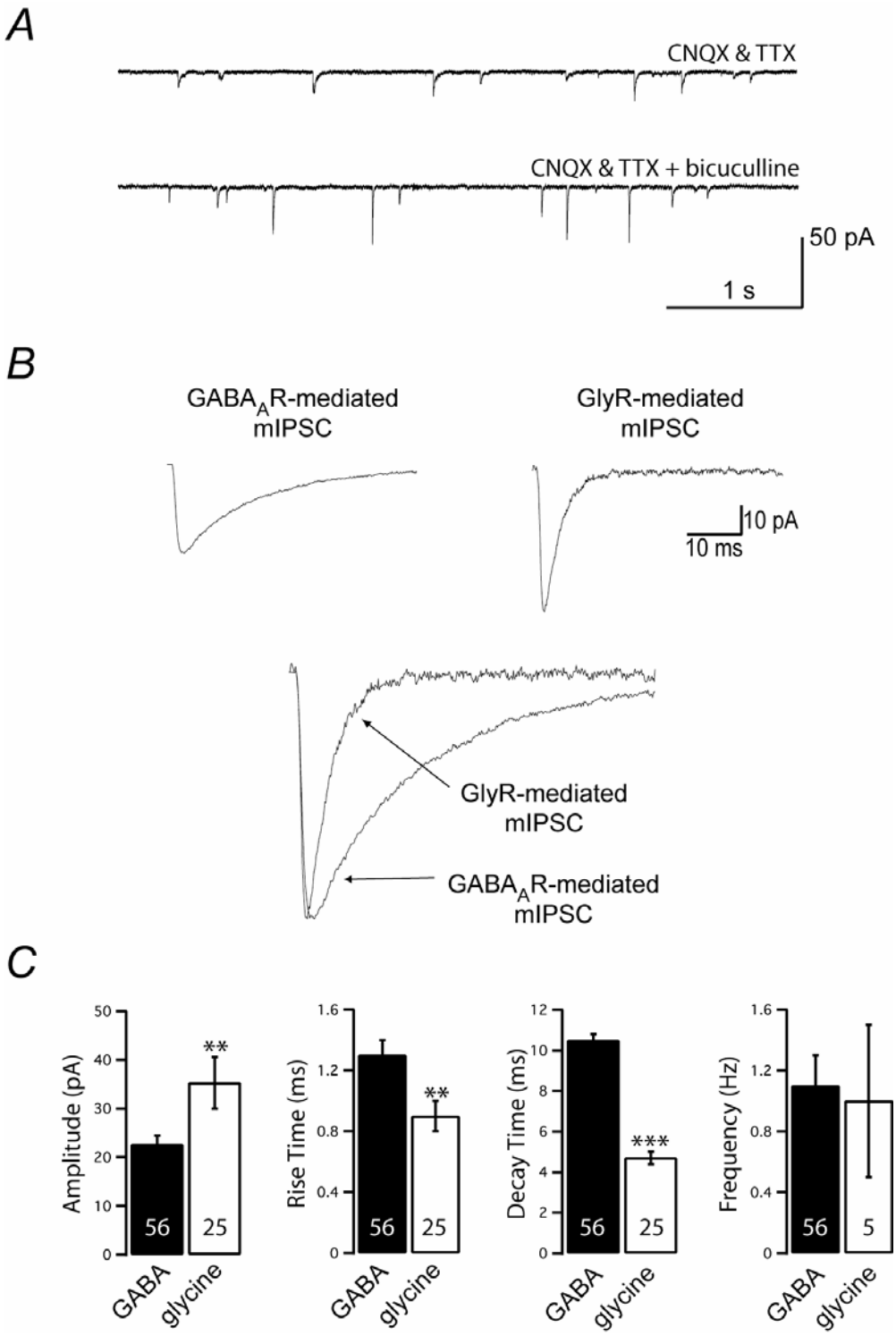

Figure 4:
Camp et al.

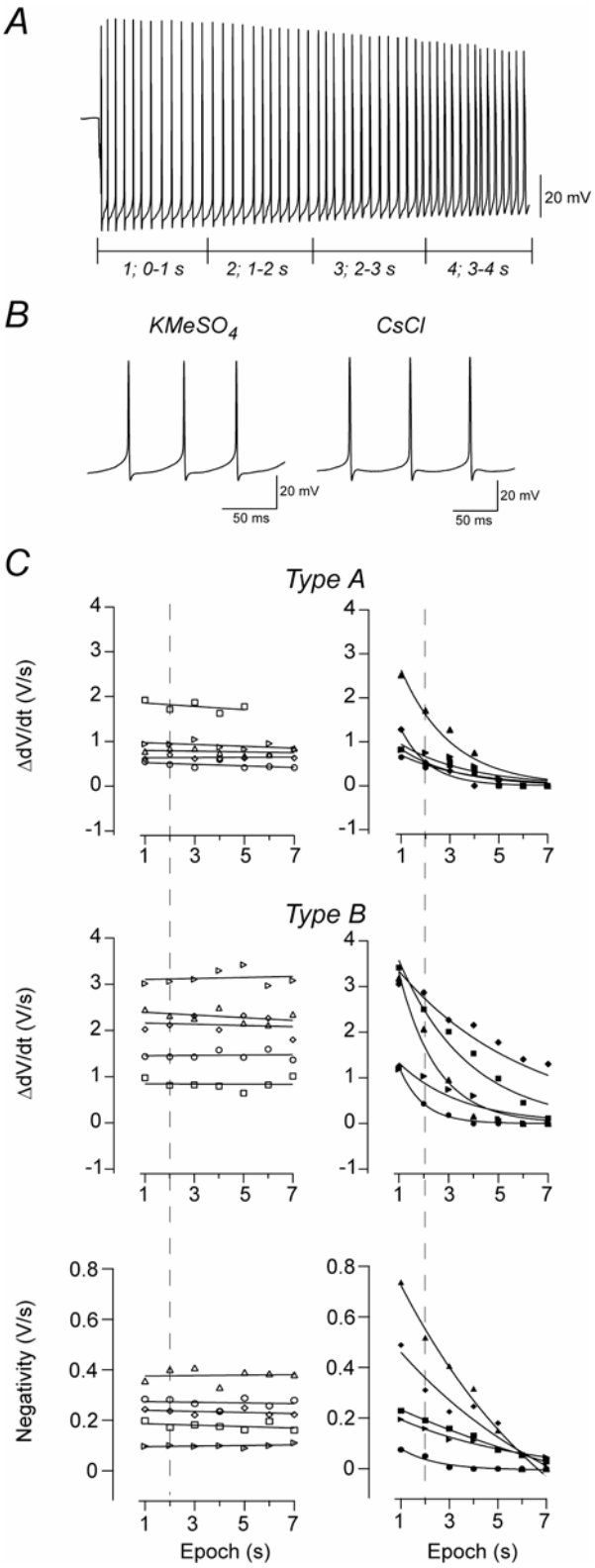

Figure 5:
Camp et al.

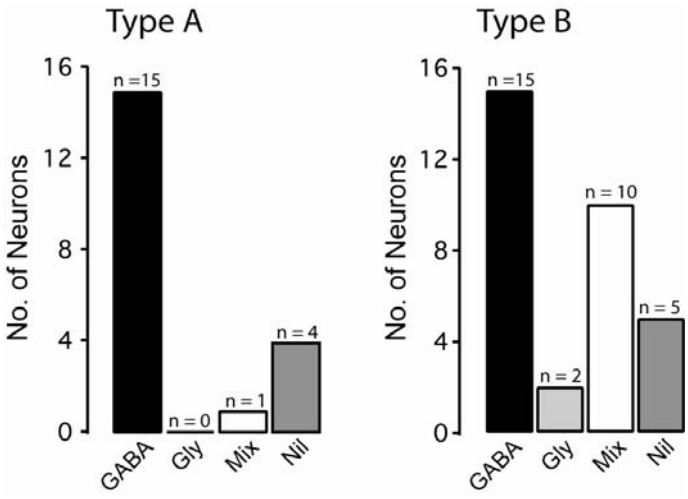

Figure 6:
Camp et al.

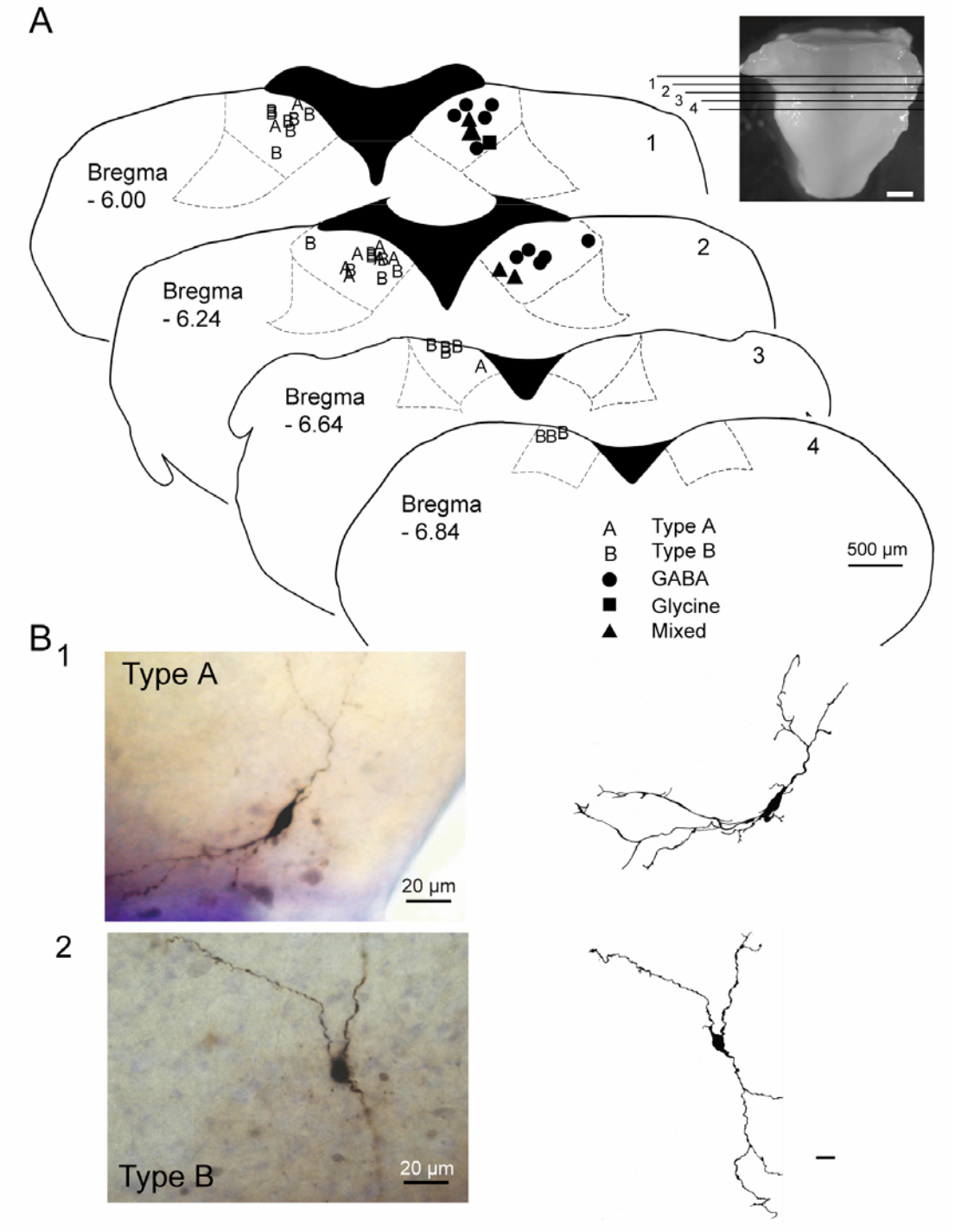

Figure 7:
Camp et al.

Table 1. $GABA_A$ergic- and glycinergic mIPSC properties in MVN neurons.

mIPSC type	Input resistance (MΩ)	Series Resistance (MΩ)	Amplitude (pA)	Rise time (ms)	Decay time (ms)	Frequency (Hz)		n
$GABA_A$	362.9 ± 29.0	15.3 ± 0.9	22.6 ± 1.8	1.3 ± 0.1	10.5 ± 0.3	1.1 ± 0.2		56
Glycine†	300.0 ± 35.7	12.1 ± 0.8	35.3 ± 5.3 **	0.9 ± 0.1 ***	4.7± 0.3 ***	1.0 ± 0.5 0.4 ± 0.1	(5)‡ (20)	25

Values are means ± SEM.
** ($P < 0.01$), *** ($P < 0.001$) indicate level of significance for differences between $GABA_A$ergic- and glycinergic mIPSC properties.
† Glycine mIPSCs isolated from both exclusively glycinergic, and "mixed" ($GABA_A$- & glycinergic) neurons.
‡ Frequency of mIPSCs in exclusively glycinergic (n=5) and "mixed" (n=20) neurons.

Table 2. Action potential properties of type A and B MVN neurons obtained using a CsCl-based internal solution.

Type	Input resistance (MΩ)	Spike Width (ms)	Amplitude (mV)	AHP Amplitude (mV)	Frequency (Hz)	n
A	301.0 ± 27.7	2.2 ± 0.2	63.7 ± 2.7	16.9 ± 1.3	29.7 ± 4.0	20
B	272.6 ± 30.2	2.1 ± 0.1	71.0 ± 2.4	13.8 ± 0.8 *	14.3 ± 1.3 ***	32

Values are means ± SEM.
* ($P < 0.05$) *** ($P < 0.001$) Significant difference between action potential properties of type A and B MVN neurons.

Table 3. Morphological properties of MVN neurons.

Type	Input resistance (MΩ)	Soma area (μm^2)	Maximum Diameter (μm)	Primary dendrites	n
$GABA_A$	276.6 ± 30.0	124.8 ± 24.7	14.6 ± 2.3	3.2 ± 0.5	10
Glycine	584	109.5	17.0	3	1
Mixed	314.8 ± 67.4	156.3 ± 31.6	19.3 ± 4.4	4.8 ± 1.3	4
A	258.3 ± 48.2	179.2 ± 27.8	21.4 ± 2.2	4.0 ± 0.5	7
B	264.2 ± 29.6	162.1 ±15.9	18.6 ± 1.6	3.9 ± 0.3	22

Values are means ± SEM.
No significant difference ($P > 0.05$) was observed between morphological properties of MVN neurons based on either inhibitory profiles or type (A or B).